SUPPLEMENTAL METHODS

Experimental Model and Subject Details

Patients

All patients and healthy controls were recruited from the Department of Dermatology at the University of Pennsylvania Hospital with appropriate Institutional Review Board approval. All subjects signed informed consent before participating in this study.

Patients were diagnosed with DM using Bohan and Peter criteria, Sontheimer criteria, or investigator expert experience and subsequently placed in a longitudinal DM database. Lesional skin biopsies were obtained from 10 patients with newly diagnosed moderate-severe DM and 5 healthy controls. The CDASI score was determined for each DM patient at time of skin biopsy. DM patients were also given the Skindex-29; this study used question 10 from the Skindex to quantify patient reported itch on a scale of 1 (never) to 5 (all the time).

Methods Details

Immunofluorescence staining

Formalin-fixed and paraffin embedded (FFPE) 4-mm skin biopsies were cut into 5-µm sections and placed onto glass slides. Slides were dewaxed at 60ºC overnight and rehydrated subsequently by washing in Citrisolv® (Fisher Scientific), 100%-50% ethanol, and deionized (DI) water. Heat induced antigen retrieval was performed in EDTA at 95ºC. Sections were blocked at room temperature (RT) for 2 hours with 3% BSA. Tissues were thereafter incubated in primary antibodies overnight at 4ºC. After washing with PBST, secondary antibody incubation was done at RT for 1hour with appropriate goat anti mouse/rabbit antibodies conjugated to Alexa

Fluor 488/594 (ThermoFisher). Tissues were washed with PBST and treated with TrueView (Vector Laboratories) for 2 minutes after which they were washed and mounted with Vector antifade mounting medium with DAPI.

RNA ISH

In situ detection of ITGAX, IFNβ, CLEC4C, IL4, IL31, and IFNγ mRNA transcripts was done using the RNAscope kit and probes (Acd Bio). Fluorescent signal amplification was used using Opal based dyes conjugated to HRP (Akoya Biosciences). Positive staining was determined to be fluorescent dots expressed higher than the negative control DapB gene from Bacillus subtilis bacterium. Slides were counterstained using DAPI and imaged using a Nikon Eclipse Ti.

IMC

Antibody Staining and Image acquisition

Prior to processing of tissue, antibodies were conjugated to different metal isotopes using the Maxpar Antibody Labeling Kit (Fluidigm). FFPE 5-µm sections were deparaffinized, washed, antigen retrieved, and blocked as above. Tissue sections were incubated in a cocktail of 37 metal conjugated antibodies in PBS with 1% BSA overnight at 4ºC with respective dilutions seen in Table S1. The next day, slides were washed in PBST and incubated with a 1:400 dilution of Intercalator- Ir (Fluidigm) for 30 minutes at RT. Slides were washed 2 times in DI water for 2 minutes each and air dried for 30 minutes afterwards. Once dried the slides were processed with the Hyperion Imaging System (Fluidigm). Regions of interest (ROI) up to 2mm x 1mm were ablated at a frequency of 200Hz.

Image processing and data analysis

The resulting MCD image files were exported to 32-bit TIFF files using MCD Viewer™ (Fluidigm). Cell segmentation was performed using a nuclear app-based algorithm in Visiopharm. The output segmentation was exported from Visiopharm and into a Cellprofiler app to create a cell mask as seen in Figure S5. The resulting mask and image TIFF files were then imported into histoCAT where per object mean pixel intensity (MPI) data was generated. The Phenograph algorithm was used for unsupervised clustering of cell populations using markers that had the best signal to noise ratio: pSTING, CD14, CD16, CD31, FOXP3, CD4, CD68, CD8, CD45RA, CD3, tryptase, CD11C, HLA-DR, MAC387, and CD163 with a second round of clustering to resolve under clustered clusters with merging phenotypes. CD20+ B cells were manually gated in FlowJo. Further subset gating for T cells was also done using CD69 and CD45RA using gate boundaries based on the corresponding image pixel values for the respective channels. Similarly, IL4 and IL31 positive mDC populations were gated in FlowJo (Figure S4). MPI for different cell populations and related heatmaps were gathered using histoCAT. Colocalization images were created using ImageJ and sliding scale pixel threshold values based corresponding marker signal/noise ratio.

Quantification and Statistical Analysis

Statistical analysis was done using GraphPad Prism v8.3. Due to small sample size and lack of normal distribution we used non-parametric tests and reported all data as median, except for average percent composition of cell populations in Figure 2b and Figure 4a. We used the Spearman rank correlation test to correlate CDASI and Skindex scores with cell counts and

pathways. The Mann-Whitney test was used to compare the HC group with DM group with $p<0.05$ being significant.

SUPPLEMENTAL TABLES

Table S1: IMC Staining Panel

Antibody	CLONE	Channel	Dilution	CAT NO
CD20	H1	115In	200	555677 (BD)
pPPARγ	polyclonal	141Pr	60	600-401-J94 (Rockland)
pSTING	D8K6H	142Nd	30	40818S (CST)
CD14	EPR3653	144Nd	200	3144025D
IL31RA	3A10	145Nd	100	H00133396-M01 (Novus)
CD16	EPR16784	146Nd	50	3146020D (Fluidigm)
CB2	polyclonal	147Sm	50	LS-A34-50 (LsBio)
IL31	polyclonal	150Nd	30	ab102750 (abcam)
CD31	EPR3094	151Eu	200	3151025D(Fluidigm)
IFNB	polyclonal	153Eu	75	NBP1-77288 (Novus)
CD45	2B11	154Sm	100	14-9457-82 (ThermoFisher)
FOXP3	236A/E7	155Gd	100	3155016D (Fluidigm)
CD4	EPRG855	156Gd	100	3156033D (Fluidigm)
CCR7	Y59	158Gd	500	ab221209 (abcam)
CD68	KP1	159Tb	150	3159035D (Fluidigm)
CD69	EPR21811	160Gd	50	ab234512 (abcam)
BDCA2	992258	161Dy	30	MAB62991-100 (RD)
CD8	C8/144B	162Dy	200	3162034D (Fluidigm)

pIRF3	polyclonal	163Dy	30	PA5-38285 (ThermoFisher)
CD56	301021	164Dy	125	14255-1-AP (Proteintech)
pTBK1	53103	165Ho	2000	ab109272 (abcam)
CD45RA	HI100	166Er	400	3166028D (Fluidigm)
IFNY	IFNG/466	167Er	50	ab218890 (abcam)
IL4	polyclonal	168Er	50	ab9622 (abcam)
IL17	polyclonal	169Tm	50	ab79056 (abcam)
CD3	polyclonal	170Er	100	3170019D (Fluidigm)
pERK	D13.14.4E	171Yb	50	3171021D (Fluidigm)
Tryptase	AA11	172Yb	20000	ab2378 (abcam)
CD11C	EP1347Y	173Yb	150	ab216655 (abcam)
HLA-DR	TAL 1B5	174Yb	400	ab20181 (abcam)
MAC387	MAC387	175Lu	800	ab22506 (abcam)
CD163	5C6-FAT	176Yb	100	MCA1853 (BioRad)

Table S2: Demographics of healthy controls and dermatomyositis patients

	HC	DM
Female n (%)	5 (100)	9 (90)
Age (y) Mean ± SD	53.8 ± 6.7	56.7 ± 4.5
Race (%)	Caucasian (100)	Caucasian (100)

Table S3: Dermatomyositis patient characteristics

Study ID	Age	Sex	Race	Site	CDASI	Skindex-29 Itch
1	74	Male	Caucasian	back	44	4
2	67	Female	Caucasian	arm	36	4
3	61	Female	Caucasian	back	30	5
4	34	Female	Caucasian	thigh	24	4
5	52	Female	Caucasian	shoulder	28	4
6	54	Female	Caucasian	back	25	2
7	62	Female	Caucasian	back	17	3
8	69	Female	Caucasian	chest	33	5
9	32	Female	Caucasian	chest	21	5
10	62	Female	Caucasian	arm	27	3

CDASI: Cutaneous dermatomyositis disease area and severity index

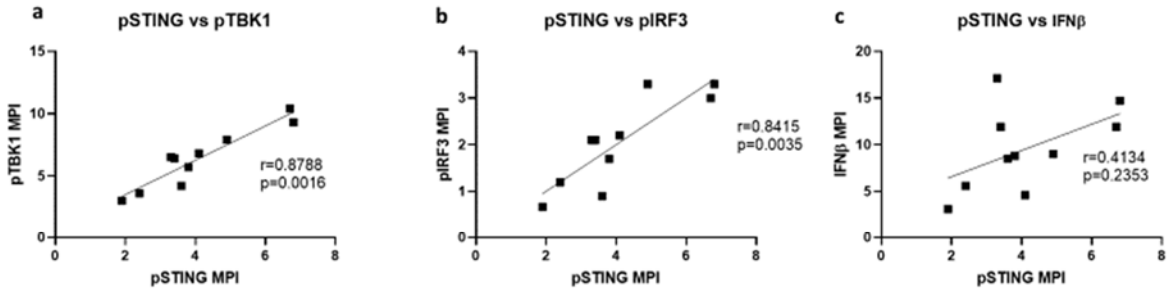

Figure S1: pSTING and downstream Type I IFN pathway correlations

a) Positive MPI per cell correlation of pSTING pathway with pTBK1
b) Positive MPI per cell correlation of pSTING pathway with pIRF3
c) No significant MPI per cell correlation of pSTING pathway with IFNβ

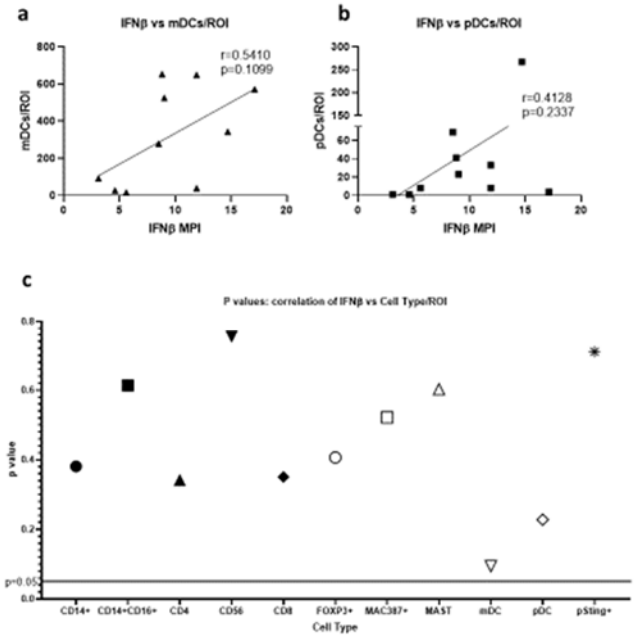

Figure S2: Correlation of the numbers of immune cells with IFNβ

a. Correlation of IFNβ with mDCs per ROI
b. Correlation of IFNβ with pDCs per ROI
c. P values for correlation of immune cells identified with IFNβ shows trend for mDCs correlating the most with overall IFNβ MPI per cell

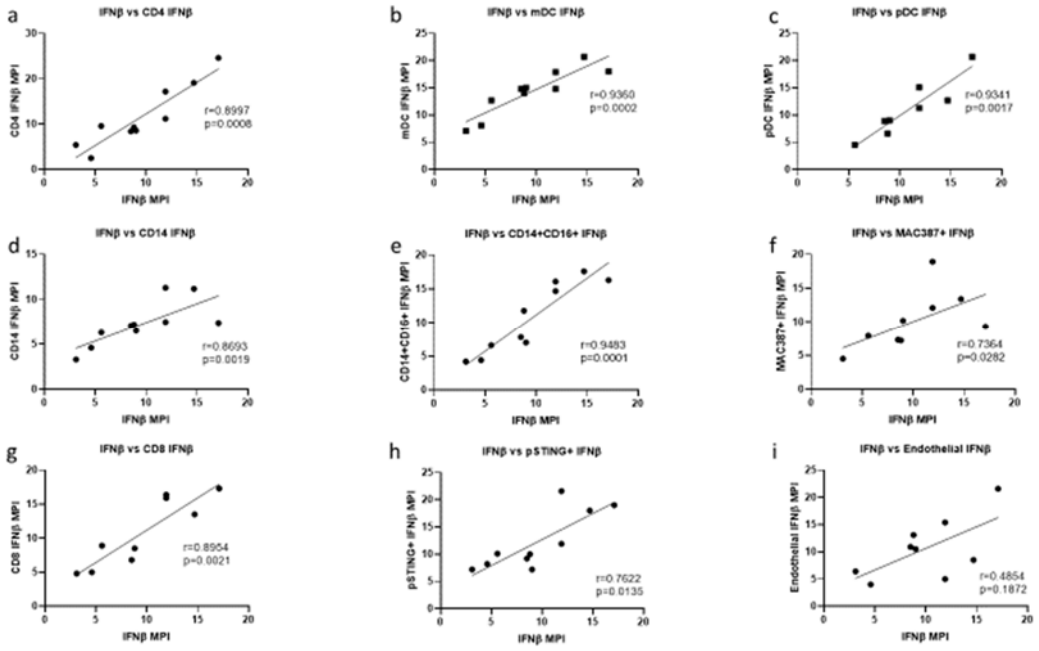

Figure S3: Overall skin IFNβ correlation with cellular IFNβ

a-h) Correlation of the overall MPI IFNβ with individual cellular IFNβ shows significant correlations for (a) CD4+ T, (b) mDCs, (c) pDCs, (d) CD14+ macrophages, (e) CD14+CD16+ macrophages, (f) MAC387+ macrophages, (i) CD8+ T cells, and (h) pSTING+ macrophages.

(i) There is no significant correlation of IFNβ with endothelial IFNβ.

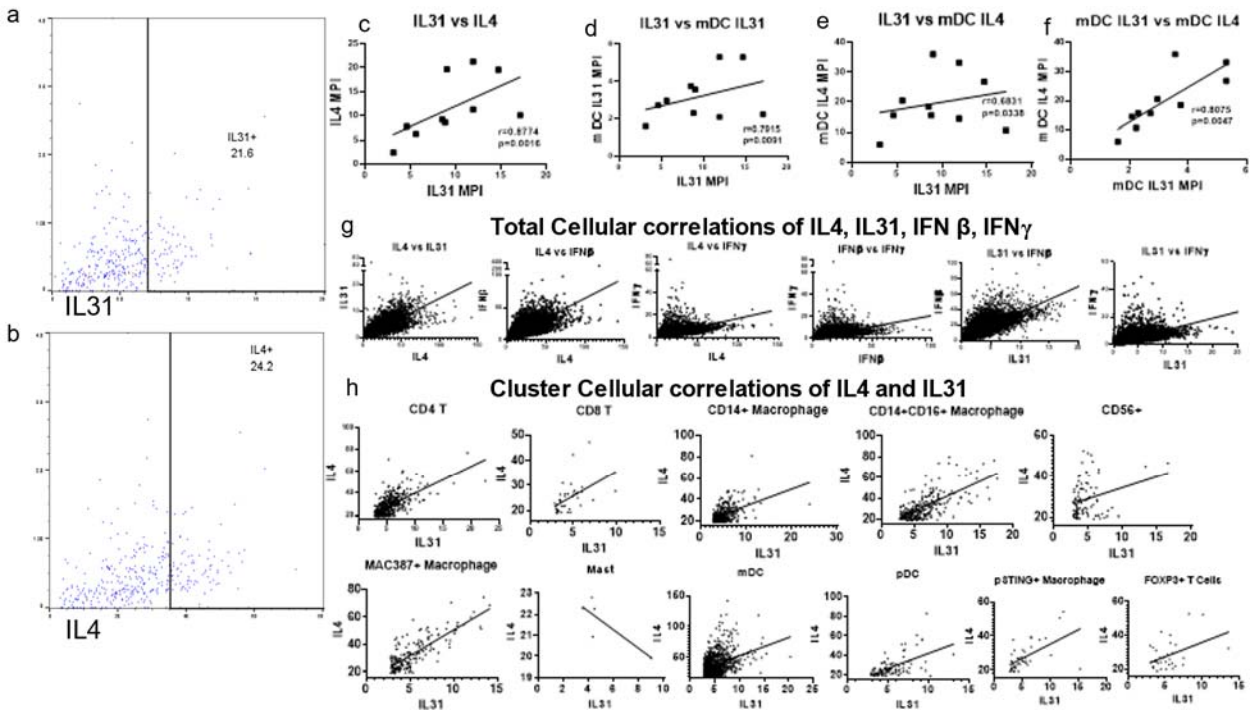

Figure S4: Gating of IL31+ and IL4+ mDCs and Correlation of IL4 and IL31 expression

a) FlowJo Gating of IL31+ mDCs

b) FlowJo Gating of IL4+ mDCs

c) Positive Correlation of overall IL31 and IL4 MPI

d) Positive correlation of overall IL31 with mDC IL31

e) Positive correlation of overall IL31 with mDC IL4;

f) Positive correlation of mDC IL31 with mDC IL4.

g) Total cellular correlation of IL4, IL31, IFNβ, and IFNy

h) Cluster Cellular correlations of IL4 and IL31

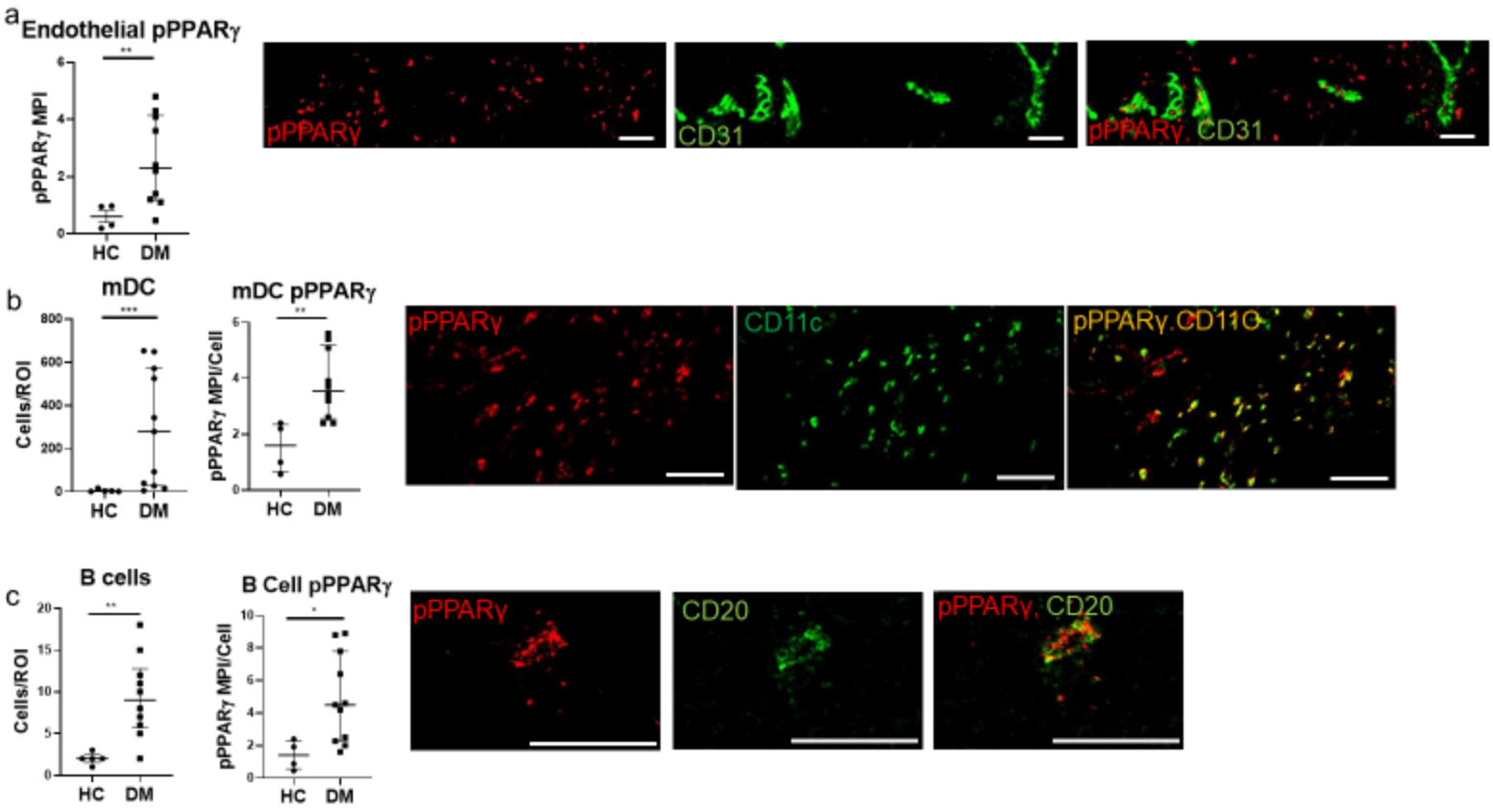

Figure S5. The Endothelium, mDCs, and B cells express increased pPPARγ in DM

a) Endothelial cells in DM skin lesions have increased pPPARγ compared to the endothelial cells in HC skin. The pPPARγ pathway (red) is upregulated in CD31+ endothelial cells (green), IMC shows colocalization of nuclear pPPARγ in endothelial cells. b) DM skin has increased mDCs compared to HC skin mDCs and they express higher levels of pPPARγ. IMC shows colocalization of pPPARγ (red) and CD11C (green) as yellow regions. c) Increased B cells in DM skin compared to HC skin also express increased pPPARγ. The pPPARγ pathway (red) is shown to overlap with B cells (green) as seen by yellow regions and intracellular location of pPPARγ. Scale bars = 100 μm (white). * $p<0.05$, ** $p<0.01$, *** $p<0.001$

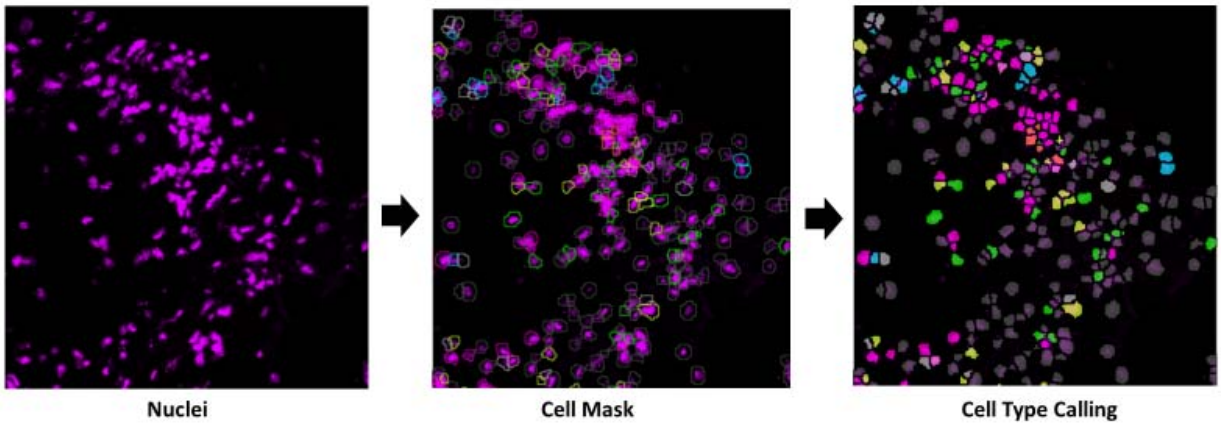

Figure S6: Nuclei based Image segmentation and cell mask creation. Segmentation of cells was performed using nuclei to create a cell mask outline which was subsequently used to identify individual cell expression profiles and cluster populations.

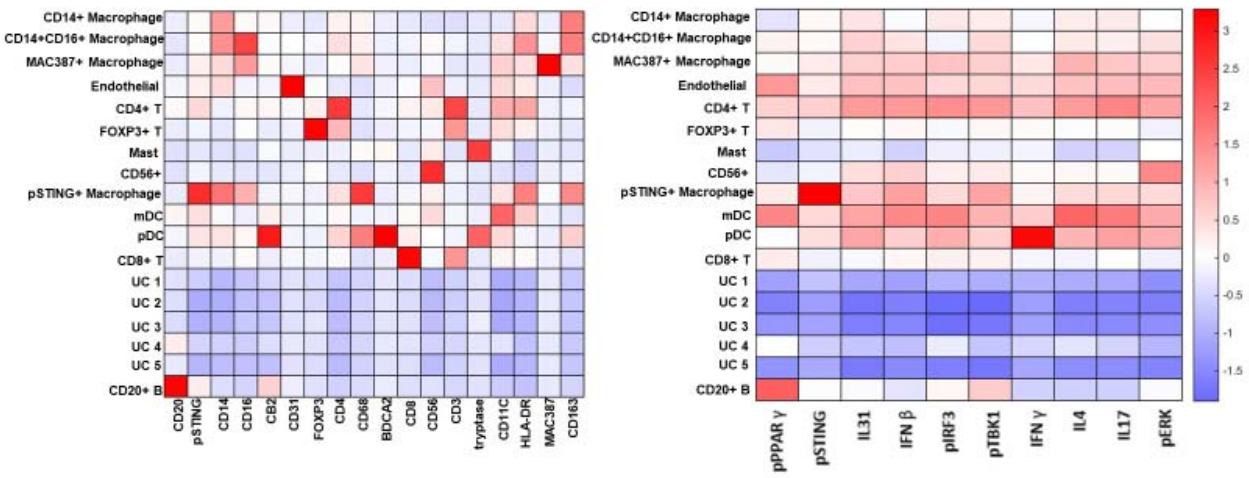

Figure S7: Heatmap of cellular and pathway markers including unidentified clusters (UC) 1-5 displaying little expression of antibodies.